Isobaric yields of near-target residues in the interaction of ^{12}C with ^{103}Rh at an incident energy of 400 MeV

E.Z. BUTHELEZI[a], K. AARDANEH[b], G.F. STEYN[a], E. GADIOLI[c], T.N. VAN DER WALT[a], F. ALBERTINI[c], M. CAVINATO[c], F. CERUTTI[c], S. H. CONNELL[d], A.A. COWLEY[e], E. FABRICI[c], S.V. FÖRTSCH[a], E. GADIOLI ERBA[c], F.M. NORTIER[f]

[a] *iThemba Laboratory for Accelerator-Based Sciences, Somerset West 7129, South Africa*
[b] *Nuclear Research Centre for Agriculture and Medicine, Karaj, Iran*
[c] *University of Milano and INFN, Sezione di Milano, Milano, Italy*
[d] *Schonland Research Centre, University of the Witwatersrand, Johannesburg, South Africa*
[e] *Department of Physics, University of Stellenbosch, Matieland 7602, South Africa*
[f] *Isotopes and Nuclear Chemistry Group, LANL, Los Alamos, USA*

Production cross sections of residues with mass near to that of the target were measured in ^{12}C induced reactions on Rh at an incident energy of about 400 MeV. Radiochemical separation of Rh and Pd from the other produced activities made it possible to accurately measure production cross sections for ^{103m}Rh and ^{103}Pd. Cross sections for the production of various other observed residues are also presented. The results are consistent with an enhanced isobaric yield in the near-target mass region.

1. Introduction

This study investigated the isobaric yields (i.e. the total cross section for production of nuclei with the same mass number) in the interaction of ^{12}C with ^{103}Rh at an incident energy of nominally 400 MeV, with particular emphasis to the target mass and the near-target mass region. This was prompted by a theoretical prediction [1] that the isobaric yield in the near-target mass region may be much larger than expectations based on older phenomenological models [2], and by as much as an order of magnitude at the target mass.

In previous studies of the excitation functions of the heavy residues produced in the interaction of α-cluster-type light nuclei (e.g. ^{12}C and ^{16}O) with nuclei, the fractions of the observed isobaric yields at or near the target mass were generally small. In the case of the ^{12}C + ^{103}Rh reaction, for example, production cross sections for only ^{103}Ag were presented [1,3], which constitutes only about 4% of the predicted isobaric yield. This lack of information at or near the target mass appears to be true in many other studies involving the interaction of a "lighter" projectile with a "heavier" target nucleus. This may be partly due to the fact that the stacked-foil activation technique usually employed to measure excitation functions (by means of off-line γ-ray spectroscopy) cannot provide data for stable nuclides or nuclides that have radiations which are difficult to measure with this technique. This includes radionuclides with low photon energies, small branching ratios, small half-lives, etc., which one often finds close to the target. However, if the target nucleus has an isomeric state only slightly above its ground state, with a half-life and radiations which make an absolute activity measurement possible, then quite a large fraction of the target isobaric yield can be experimentally determined.

Since ^{103}Rh has an $7/2^+$ isomeric state (normally designated as ^{103m}Rh) which is only 39.76 keV above the ground state, this nucleus should be a convenient target for the present study. Futhermore, the measurement of the cumulative cross sections of the relatively long-lived ^{103}Pd (16.96 days) and ^{103}Ru (39.25 days) [4] together with the cross section for the direct production of ^{103m}Rh (56.12 minutes) should constitute more than 80% of the predicted

A = 103 isobaric yield. In addition, the relative strengths of these nuclides may also constitute a sensitive test of the predictive power of the theoretical models employed to interpret the data. Thus, production cross sections for the A = 103 radionuclides, even if measured at only one well-chosen incident energy, may be sufficient to either confirm or disprove an enhanced isobaric yield.

The experimental determination of production cross sections for ^{103}Pd, ^{103m}Rh and ^{103}Ru proved to be non-trivial. Both ^{103}Pd and ^{103m}Rh only have very weak γ-lines, therefore the only feasible way to obtain their activities would be to measure the 20.1 keV K_α x-rays [4] (63.8% and 6.37%, respectively). But many of the other nuclides produced in these reactions have x-ray lines in the same energy region (i.e. about 19-22 keV) which would interfere with these measurements. The radiochemical separation of the different atomic species will therefore be a requirement. Furthermore, ^{103m}Rh is an isotope of the same species as the target. A comprehensive radiochemical purification of the target material from all the other disturbing radionuclides is required before an absolute yield measurement for this nuclide can be performed. The relatively small half-life of just under one hour (56.12 minutes) is a further complication since the chemical separation and production of suitable counting sources have to be rapid processes. The relatively long-lived ^{103}Ru, by contrast, has strong γ-lines but it is produced in only minute amounts in the reaction investigated.

Both ion exchange chromatography and solvent extraction methods have been used for the separation of Pd from Rh and other elements [5-13] but none of these have fulfilled the requirements for this particular study, i.e. the isolation of Rh from Ag, Pd, Ru and Tc, followed by the separation of Pd from the rest of the elements. Note that Ag and Pd are the two nearest atomic species above Rh, while Ru and Tc are the two nearest ones below Rh in the periodic table. These elements, in particular, need to be separated from the Rh target material in order to accurately measure the 20.1 keV K_α x-rays emitted in the decay of ^{103m}Rh. A radiochemical method which utilises the strongly basic anion exchange resin AG1-X8 with 6 M HCl as the eluent was consequently developed as part of this study [14].

In this work we present measured cross sections for the cumulative production of ^{103}Ag, ^{103}Pd and ^{103}Ru, and for the direct production of ^{103m}Rh at an incident energy of nominally 400 MeV. In addition, we also present the values for many other radionuclides which we could identify from their respective γ-lines in an attempt to reconstruct as much of the total isobaric mass-yield curve in as large a mass region as possible.

2. Experimental methods

Target preparation and irradiations

Metallic Rh is very inert and therefore difficult to dissolve to obtain it into a solution. The need to rapidly dissolve the target material after irradiation, as required by the radiochemistry, precluded metallic rhodium for this purpose. We therefore irradiated both metallic foils and compressed Rh-chloride disks in this experiment, the latter solely for the purpose of measuring production cross sections of nuclides which cannot be determined by means of off-line γ-ray spectroscopy of intact metallic foils.

Thin disks (15 mm in diameter and 79 mg/cm^2 thick) of high-purity $RhCl_3.xH_2O$ were produced by powder compaction in a hydraulic press. This material was found to readily dissolve in hydrochloric acid.

The irradiations were performed at the cyclotron facility of the iThemba Laboratory for Accelerator-Based Sciences (formerly known as the National Accelerator Centre), Somerset West, South Africa. The beam energy as determined from a calibrated 90° analysis magnet was 394.5 MeV with an overall uncertainly of about 1 MeV. Two $RhCl_3$ disks were

irradiated – the first for 1 hour to determine the shorter-lived radionuclides and the second for 5 hours to determine the longer-lived nuclides. The disks fitted tightly inside a small recess machined into one face of a water-cooled copper beam stop, which again fitted inside a small Faraday chamber mounted directly onto an external beamline. A thin 5 μm Ti foil served as a window for the target assembly to protect the target disk, maintain the integrity of the vacuum during irradiation and also to serve as a beam monitor for a consistency check on the current integration. The beam current of nominally 50 nA was integrated and logged every 10 seconds. The Faraday chamber was well insulated electrically from the beamline and all surrounding structures, and electron suppression by means of permanent magnets was provided at the chamber entrance. This ensured that the accumulated charge could be accurately measured with an uncertainty of less than 2%.

A single stack of metallic Rh foils were also irradiated with the ^{12}C beam. The stack consisted of a single 5 μm Ti monitor foil, followed by several Rh foils of nominally 32 mg/cm^2 thickness. The stack thickness was such that it stopped the beam.

Radiochemical separations

Details of the radiochemical separation techniques employed will be presented elsewhere [14]. Here it will suffice to mention that three kinds of solutions were obtained from which dry counting sources were prepared: (1) the mother solution, i.e. the solution obtained by dissolving an irradiated Rh-chloride target; (2) the Rh solution, i.e. a solution containing only the separated Rh isotopes, and (3) the Pd solution, i.e. a solution containing only the Pd isotopes.

Preparation of counting sources

Counting sources were prepared from the three kinds of solutions mentioned above by evaporating accurately-measured quantities of solution to dryness in small PVC source holders under an infrared lamp.

Following the short (1h) irradiation, four sources were prepared - two from the mother solution and two from the Rh-solution. Similarly, four sources were prepared after the long (5h) irradiation - two from the mother solution and two from the Pd-solution. In each case, a quantity of 1 ml of the particular solution was transferred to the source holder and evaporated to dryness. In total, therefore, 8 of these sources were prepared for the experimental measurements.

Suitable calibration sources with the same geometry as the experimental sources were prepared from standardised ^{133}Ba, ^{152}Eu and ^{241}Am solutions. These calibration sources were prepared, especially for this experiment, by the CSIR National Metrology Laboratory in Cape Town, South Africa, traceable to the BIPM in Sèvres, France.

Radionuclide assays

Two accurately calibrated HPGe detectors, coupled to a 16k channel SILENA multi-channel analyser system, were used. One detector was a standard EG&G ORTEC coaxial intrinsic Ge γ-ray detector with a crystal diameter of 53 mm and 64 mm thickness. The other was an APTEC planar Ge *x*-ray detector with an active area of 200 mm^2 and a thickness of 10 mm. Both detectors had horizontal configurations and source holders moving on rails to optimise the source-detector distance. The resolution was 1.7 keV FWHM at 122 keV for the γ-ray detector and 0.92 keV FWHM at 21 keV for the *x*-ray detector. The two detectors were properly separated and shielded from each other.

The reason why two sources of each kind with identical strengths were prepared was to simultaneously collect γ-ray and *x*-ray spectra in order to optimise our data taking. The counting of the Rh sources started about 80 minutes after EOB and they were counted repeatedly to follow the decay as a function of time. The Pd sources were counted a few days later since ^{103}Pd has a relatively long half-life. All sources were also re-counted at later times, after the decay of the shorter-lived radionuclides, in order to more accurately assay the longer-lived radionuclides. This provided various cross-checks for the consistency of the data and also served to quantify contaminants in the final solutions obtained from the chemical separations. Although the levels of radiocontamination in the final solutions were generally small, they were not negligible and appropriate corrections to the data were subsequently made. Losses incurred in the chemical separations were also carefully quantified and appropriate corrections were made.

In the case of the metallic Rh foils, only γ-ray spectra were collected. Cross sections were calculated from the measured activities for all the radionuclides identified in these spectra. The foils were counted several times during four counting sessions: shortly after EOB, several hours after EOB, two weeks after EOB and again one month after EOB.

3. Theoretical Considerations

Quite a large number of activation measurements of the formation cross sections of residues in reactions of light and medium-mass ions with nuclei can be found in the literature. Among these are of particular interest for us those concerning the interaction of 15 to 45 MeV/amu ^{12}C ions with natural silver [2] and natural copper [15,16]. In those experiments, a significant fraction of the yield of near-target residues could not be measured. Furthermore, the data were analysed using the hypothesis that the percentage charge distribution (PCD) of the isobars produced in the reaction could be accurately represented by a quasi-Gaussian distribution, almost independent of their mass and the total cross section for their production. This procedure was first suggested by Rudstam [17] in the analysis of a large number of reactions induced by protons and, in a smaller number of cases, by deuterons and α-particles.

In Refs. [2,15,16] the formation cross sections of residues were calculated using the following ten-parameter formula:

$$\sigma(A,Z) = \exp[\alpha_1 + \alpha_2 A + \alpha_3 A^2 + \alpha_4 A^3 + (\alpha_5 + \alpha_6 A + \alpha_7 A^2) \mid Z_p - Z \mid^{\alpha_8}], \quad (1)$$

where

$$Z_p = \alpha_9 + \alpha_{10} A. \quad (2)$$

The parameters α_1 through α_4 largely determine the shape of the mass-yield distribution, while α_5 through α_7 determine the width of the isobaric charge distribution. The parameter α_8 determines the shape of the isobaric charge distribution, which corresponds to a Gaussian when $\alpha_8 = 2$. The isobaric charge distribution is assumed to be symmetric about a most-probable charge Z_p, which has a linear mass dependence as given by equation (2). Values for the parameters are found by means of an iterative least-squares fit procedure to existing data. Equation (1) is then used to deduce the values of the cross sections for production of unobserved residues. However, with increasing incident energy the average forward recoil ranges of the residues measured in these experiments display a significant mass dependence. The typical range of a residue with mass similar to that of the target is very small, while that of a residue with significantly smaller mass is considerably larger. This implies that notably different reaction mechanisms are involved in the production of near-target and far-target

residues, while the use of similar PCDs seems to be justified only for quite similar production mechanisms. This paradox, which is common in the analysis of several other experiments of this type, was not explained.

In our previous studies of the production cross sections and recoil range distributions of residues in the interaction of ~5 to ~35 MeV/amu ^{12}C ions with ^{103}Rh [1,3] we also found that the near-target residues have on average a very small range, i.e. very small linear momentum and we hypothesized that these residues are produced by particular mechanisms implying a small energy and mass deposition in the target nucleus. Thus, the cross sections for production of a large number of residues in the irradiation of ^{103} Rh both with ^{12}C and ^{16}O at energies varying from about 60 to 400 MeV were quite successfully interpreted by considering the contributions of the following quite different reaction mechanisms: (i) complete fusion; (ii) incomplete fusion of α-like fragments produced in the break-up of the projectile (i.e. single α particles and ^{8}Be fragments, and in the case of ^{16}O induced reactions, also ^{12}C fragments); (iii) and single-nucleon transfer from the projectile to the target. The incomplete fusion reactions were described as break-up-fusion processes, i.e., binary fragmentations of the projectile followed by the absorption of one of the fragments by the target nucleus. The mean field interaction (one-body dissipation mechanism) was considered to rule the fragmentation mechanism. The energy and angular distributions of the fragments were evaluated in the local plane wave approximation [18], i.e. reducing the kinetic energy of the projectile by the coulomb repulsion of the target at the break-up location and using the Serber theory [19] to evaluate the fragment double differential spectra.

The nuclei produced in both the complete and incomplete fusion reactions, the intermediate excited nuclei (IEN), are initially in a state far from equilibrium and were assumed to progress toward the state of statistical equilibrium by means of an intranuclear interaction cascade, described by means of the Boltzmann Master Equation theory. During this cascade, pre-equilibrium emission of particles and particle aggregates may occur [20,21].

Another mechanism which was considered was the re-emission of absorbed α particles after a few interactions with the target nucleons [22,23]. This mechanism, as well as the single-nucleon transfer reactions, produce only slightly excited IEN which in their subsequent decay may at most emit a few particles. Quite a considerable fraction of the reaction cross section was therefore predicted to lead to the formation of near target residues. As was mentioned in the Introduction, the cross sections for production of many of these residues could not be measured in these previous works and this prediction could not be experimentally tested. However, it was considered to be realistic because the same approach allowed one to reproduce quite satisfactorily both the measured cross section of residues with mass not much different from that of the target as well as their recoil range properties. In these works, the cross sections for both complete and incomplete fusion reactions and also nucleon transfer processes were evaluated in the framework of the entrance-channel critical angular momentum model [24-26].

Further experiments, in which the spectra of the fragments produced in the binary fragmentation of the projectile were measured, led us to modify some of the hypotheses made previously [27-30]. The main results of that series of experiments are: (i) other break-up modes of the projectile also need to be considered (e.g. $^{7}Li + ^{5}Li$ and $^{6}Li + ^{6}Li$, $^{5}He + ^{7}Be$ and $^{3}He + ^{9}Be$ in the case of ^{12}C projectiles and $^{10,11}B + ^{6,5}Li$ and $d + ^{14}N$ in the case of ^{16}O projectiles); (ii) the cross sections for α and single-nucleon transfer could be better estimated (in particular the cross section for α transfer was found to be considerably less than previously estimated); (iii) and perhaps the most important finding was that at incident energies exceeding 200 MeV, both ^{12}C and ^{16}O were found to suffer a quite considerable energy loss in an initial-state interaction by means of a kind of friction mechanism which excites the target nucleus. This energy loss has a quite remarkable effect on the evaluation of

the cross sections of near-target residues because even in the case of incomplete α particle absorption followed by α re-emission, the IEN now have a sizeable excitation energy. They may therefore emit several particles in their subsequent de-excitation, thus producing nuclei of mass considerably smaller than that of the target nucleus. This effect is partially compensated by the inelastic scattering of the projectile which, in agreement with the new findings, was found to be more important than previously suspected.

The present theoretical analysis of the cross sections of the residues observed in several previous experiments as well as in this experiment, reproduce these experimental cross sections only slightly better than previous calculations. However, a great advantage of our present analysis approach is that a large set of data which previous calculations could not reproduce, can now also be reproduced satisfactorily [31]. The indication that a considerable fraction of the reaction cross section leads to the formation of near target residues is still true.

4. Results and Discussion

Figure 1 (a) shows a typical *x*-ray spectrum of a source prepared from one of the mother solutions, while Fig. 1 (b) shows the corresponding spectrum obtained from the Rh solution. Clearly, without any radiochemistry the 20.1 keV K_α yield cannot be uniquely determined. In contrast, completely resolved photopeaks were obtained from the Rh and Pd sources prepared during the radiochemical separation procedures.

Since the cross sections were extracted from rather thick targets, they represent *average* cross sections. The ^{12}C beam energy loss in a $RbCl_3$ disk was nominally 39 MeV, therefore all calculations were performed for a nominal projectile energy of 380 MeV. The choice of the $RhCl_3$ target thickness was a compromise between conflicting requirements. On the one hand the time constraints allowed for only small volumes to be evaporated to dryness in the preparation of the counting sources. On the other hand, sufficiently strong sources were needed for the radionuclide assays, therefore a relatively large quantity of target material had to be activated with a rather low beam intensity to avoid damage to the targets while simultaneously providing enough activity. The choice of the beam energy of ~400 MeV has an important advantage in that it is significantly above the thresholds of most of the contributing reaction mechanisms. In fact, the shapes of the excitation functions of the majority of the observed residues are quite flat and structureless in the energy region 360-400 MeV (see e.g. Ref. 3), therefore large differences between the average cross sections extracted and the values evaluated at the nominal projectile energy of 380 MeV are not expected.

Figure 2 shows the comparison between the measured cross sections (solid points) and the corresponding theoretical predictions (dotted histogram) for those residues that have the largest cross sections at a particular mass. In a few cases where both the ground state and a metastable state have been measured for the same nuclide and the metastable state does not significantly feed the ground state, the sum of the two contributions were taken. The experimental values plotted are best values, therefore often derived from the spectra obtained from the metallic stack irradiations. In order to present a consistent set of results, all the values were averaged over the energy window corresponding to the thickness of a $RhCl_3$ disk. The agreement is reasonable except for a possible underprediction below $A = 90$ which may be in part due to an approximation which we made for simplifying the calculation, i.e., the neglecting of the emission of intermediate mass fragments during the thermalization cascade which indeed our theory predicts [29,30]. Clearly, the experimental data are consistent with an enhanced isobaric yield in the near-target mass region. At several masses the observed isobaric yield comprises a significant fraction of the predicted total, as shown by the solid histogram.

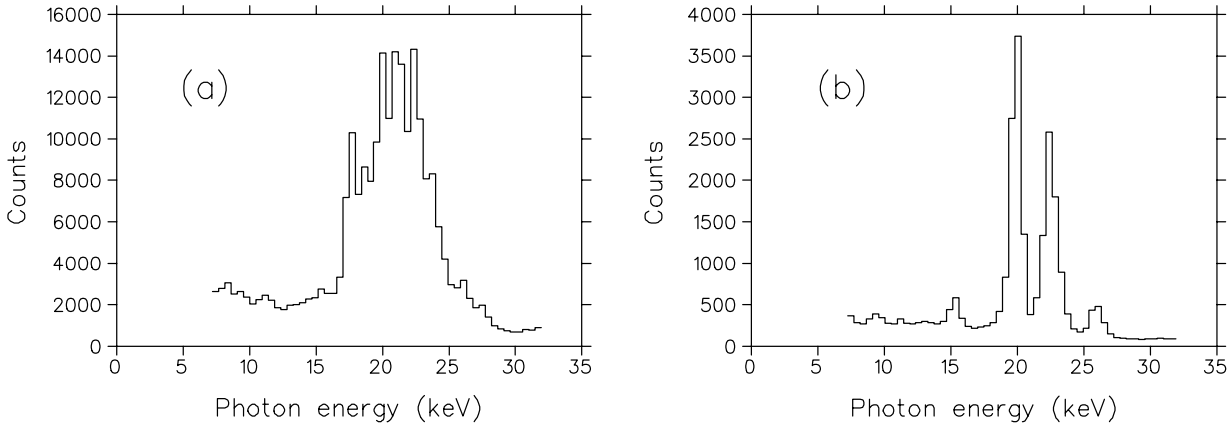

Fig. 1. A typical *x*-ray spectrum of a source prepared from the mother solution, i.e. before any radiochemistry, is shown in (a) and the corresponding spectrum from the Rh solution, i.e. after radiochemistry, is shown in (b).

Figure 3 compares the isobaric yield distribution for $^{12}C + ^{103}Rh$ predicted by our theory with a prediction according to the phenomenological expressions given by equations (1) and (2) with the parameters of Table 1. It is evident that the phenomenological prediction underestimates the isobaric mass-yield in the near-target region. In the mass region below about $A = 100$ and above $A = 103$, however, a reasonable agreement could be found.

Table 1
Parameter values obtained from least-squares fits of equations (1) and (2) to available data.

α_1: 26.9	α_2: -2.83	α_3: 5.2×10^{-2}	α_4: -2.6×10^{-4}	α_5: -1.56
α_6: 4.25×10^{-3}	α_7: 3.54×10^{-5}	α_8: 1.85	α_9: 0.49	α_{10}: -4.62×10^{-4}

5. Conclusions

Experimental cross sections for the production of target-like residues, with particular emphasis on the near-target mass region, have been presented for the reaction $^{12}C + ^{103}Rh$ at an incident energy of ~400 MeV. The results are consistent with an enhanced isobaric yield in the near-target mass region. The agreement with theoretical predictions based on a comprehensive theory which is being developed by some of the present authors, is reasonable. In contrast, phenomenological predictions underestimate the isobaric yield in the near-target mass region. Neglecting to consider the enhanced production of near target residues may lead to underestimating the total reaction cross section to a notable extent and to overestimating the mass and energy transfer from the projectile to the target. Thus, the results of analyses of light-ion induced reactions based on the use of phenomenological expressions such as presented by Rudstam (or derivations thereof) should be considered cautiously.

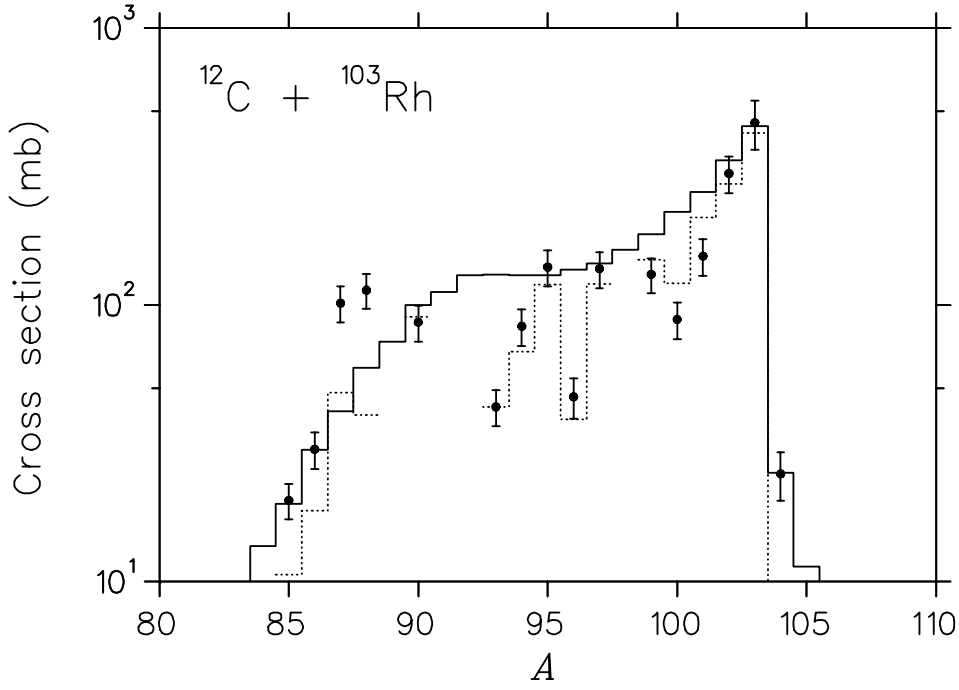

Fig. 2. The solid points are the measured production cross sections of those residues observed with the largest cross section at a particular mass in the interaction of ^{12}C with ^{103}Rh at a nominal energy of 380 MeV. The dotted histograms are the corresponding theoretical predictions. The solid histograms are the respective total isobaric yields predicted by the same theory (see text).

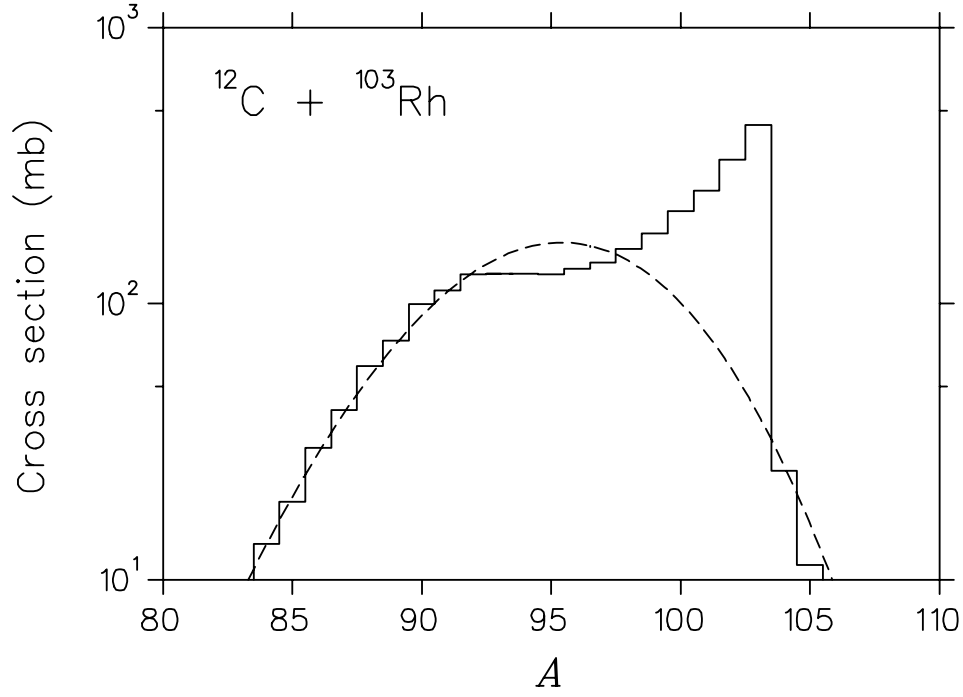

Fig. 3. The histogram is the total isobaric yield predicted by our theory for $^{12}C + ^{103}Rh$ at an incident energy of 380 MeV, while the dashed curve is a prediction based on a phenomenological model originally proposed by Rudstam (see text).

References

1. E. Gadioli, C. Birattari, M. Cavinato, E. Fabrici, E. Gadioli Erba, V. Allori, C. Cerutti, A. Di Filippo, S. Vailati, T.G. Stevens, S.H. Connel, J.P.F. Sellschop, F.M. Nortier, G.F. Steyn, C. Marchetta, Nucl. Phys. **A 641** (1998) 271.
2. Y.H. Chung, S.Y. Cho, N.T. Porile, Nucl. Phys. **A 533** (1991) 170.
3. E. Gadioli, C. Birattari, M. Cavinato, E. Fabrici, E. Gadioli Erba, V. Allori, C. Bovati, F. Cerutti, A. Di Filippo, E. Galbiati, T.G. Stevens, S.H. Connel, J.P.F. Sellschop, S.J. Mills, F.M. Nortier, G.F. Steyn, C. Marchetta, Phys. Lett. **B 394** (1997) 29.
4. E. Browne, R.B. Firestone, Table of Radioactive Isotopes (ed. V.S. Shirley), John Wiley and Sons, U.S., 1986.
5. R. Gaita, S.J. Al-Bazi , Talanta **42** (1995) 249.
6. M.C. Lagunas-Solar, M.J. Avila, P.C. Johnson, J. Appl. Radiat. Isot. **35** (1984) 743.
7. F.W.E. Strelow, T.N. van der Walt, S. Afr. J. Chem. **34** (1981) 50.
8. A. Hermanne, M. Sonck, S. Takacs, F. Tarkanyi, Y. Shubin, Nucl. Instr. and Meth. **B 187** (2002) 3.
9. J. Lingen, H. Yan, Chinese Journal of Reactive Polymers **1** (1992) 54.
10. P. Tarapcik, V. Mikulaj, Radiochem. Radioanal. Lett. **48** (1981) 15.
11. S.P. Patil, V. M. Shinde, Mikrochimica Acta **12** (1974) 853.
12. A.K. Chakkar, L.R. Kakkar, Fresenius J. Anal. Chem. **338** (1990) 79.
13. V. Mikulaj, F. Macasek, P. Rajec, J. Radioanal. Chem. **51** (1979) 55.
14. E.Z. Buthelezi et al., J. Radioanal. Nucl. Chem*, to be submitted*.
15. S.Y. Cho, Y.H. Chung, N.T. Porile, D.J. Morrissey, Phys. Rev. **C 36** (1987) 2349.
16. S.Y. Cho, N.T. Porile, D.J. Morrissey, Phys. Rev. **C 39** (1989) 2227.
17. G. Rudstam, Z. Naturforsch. **A 21** (1966) 1022.
18. K. W. McVoy, M. Carolina Nemes, Z. Phys. **A 295** (1980) 177.
19. R. Serber, Phys. Rev. **72** (1947) 1008.
20. M. Cavinato, E. Fabrici, E. Gadioli, E. Gadioli Erba, E. Risi, Nucl. Phys. **A 643** (1998) 15.
21. M. Cavinato, E. Fabrici, E. Gadioli, E. Gadioli Erba, G. Riva, Nucl. Phys. **A 679** (2001) 753.
22. E.Gadioli, E.Gadioli Erba, M.Luinetti, Zeitschrift f. Physik A321 (1985) 107
23. E. Gadioli, M. Cavinato, E. Fabrici, E. Gadioli Erba, C. Birattari, I. Mica, S. Solia, G. F. Steyn, S.V. Förtsch, J.J. Lawrie, F.M. Nortier, T.G. Stevens, S.H. Connell, J.P.F. Sellschop, A.A. Cowley, Nucl. Phys. **A 654** (1999) 523.
24. J. Wilczyński, Nucl. Phys. **A 216** (1973) 386.
25. D. Glas, U. Mosel, Nucl. Phys. **A 237** (1975) 429.

26. K. Siwek-Wilczyńska, E.H. Du Marchie van Voorthuizen, J. van Popta, R.H. Siemssen, J. Wilczyński, Nucl. Phys. **A 330** (1979) 150.

27. E. Gadioli, M. Cavinato, E. Fabrici, E. Gadioli Erba, R. Bassini, C. Birattari, S. Crippa, G.F. Steyn, S.V. Förtsch, J.J. Lawrie, F.M. Nortier, S.H. Connell, E. Sideras Haddad, J.P.F. Sellschop, A.A. Cowley, Eur. Phys. J. **A 8** (2000) 373.

28. E. Gadioli, G.F. Steyn, C. Birattari, M. Cavinato, S.H. Connell, A.A. Cowley, E. Fabrici, S.V. Förtsch, E. Gadioli Erba, J.J. Lawrie, F.M. Nortier, J.P.F. Sellschop, E. Sideras Haddad, Eur. Phys. J. **A 11** (2001) 161.

29. E. Gadioli, G.F. Steyn, C. Birattari, C. Catarisano, M. Cavinato, S.H. Connell, A.A. Cowley, E. Fabrici, S.V. Förtsch, E. Gadioli Erba, J.J. Lawrie, J.P.F. Sellschop, E. Sideras Haddad, Nucl. Phys. **A 708** (2002) 391.

30. E. Gadioli, G.F. Steyn, F. Albertini, C. Birattari, M. Cavinato, S.H. Connell, A.A. Cowley, E. Fabrici, S.V. Förtsch, E. Gadioli Erba, J.J. Lawrie, M. Pigni, J.P.F. Sellschop, E. Sideras Haddad, Eur. Phys. J. **A17** (2003) 195.

31. E. Gadioli et al., *to be published.*